Paper D

Model Predictive Control of a Norske Skog Saugbrugs Paper Machine: Preliminary Study

Hauge, T.A., Slora, R. and Lie, B. (2002). *Model Predictive Control of a Norske Skog Saugbrugs Paper Machine: Preliminary Study*, in proceedings of Control Systems 2002, June 3-5, Stockholm, Sweden, p 75-79.

Extended version.

Model Predictive Control of a Norske Skog Saugbrugs Paper Machine: Preliminary Study

Tor Anders Hauge*, Roger Slora†, and Bernt Lie‡

Abstract

In this paper we give an overview of some of the work, carried out in a project at Norske Skog Saugbrugs in order to stabilize the wet end of paper machine 6 (PM6). A nonlinear physical based model was developed and will be used in a model predictive control (MPC) application. Results from a controllability analysis is given, indicating the necessity of process operators acting on measured disturbances to avoid input saturation. A commercially available MPC algorithm based on a linear model is modified to handle the nonlinear model, and to allow for future setpoint changes.

1 Introduction

A project for stabilizing the wet end of paper machine 6 (PM6) at Norske Skog Saugbrugs was initiated in late 1999 (see e.g. (Hauge, Ergon, Forsland, Slora & Lie 2000)), and the project will continue throughout 2002. The present state of the project for stabilizing the wet end, is that a process model has been developed, fitted, and validated with mill data (Hauge & Lie 2002). The model is implemented in a commercially available MPC solution, and the vendor of this MPC is currently modifying the software based on inputs from PM6 engineers. In addition to implementing an MPC, several single-input single-output control loops and feed forward controllers are implemented at PM6 for stabilizing variables outside the scope of the MPC.

This paper is organized as follows. In Section 2 we briefly outline the preprocessing of data carried out before the model was fitted. The model is described and some fitting and validation results are discussed in Section 3. In Section 4 we analyze and discuss controllability (the ability to achieve acceptable control performance). The APIS software and APIS MPC is described in Section 5, and a simulation result is shown in Section 6. Finally, in Section 7, some conclusions are given.

*Telemark University College, P.b. 203, 3901 Porsgrunn, Norway. E-mail: Tor.A.Hauge@hit.no
†Norske Skog Saugbrugs, 1756 Halden, Norway. E-mail: Roger.Slora@norske-skog.com
‡Telemark University College, P.b. 203, 3901 Porsgrunn, Norway. E-mail: Bernt.Lie@hit.no

2 Preprocessing the data

When analyzing controllability we need to know something about the frequencies where the model is valid. An important aspect is the preprocessing of data which is discussed in this section.

The raw data collected from the paper machine has sampling rates of 5 s or 10 s. Those data sets having a sampling rate of 10 s are transformed into 5 s sampling rates by linear interpolation. The data have high frequency disturbances, particularly in the output variables: basis weight and paper ash. These disturbances have higher frequencies than the frequencies of interest, and we low-pass filter all data, prior to model fitting and identification, to put less weight on higher frequencies. All input and output series with 5 s sampling rate are filtered through a second order Butterworth filter

$$v_{\text{filtered}} = \frac{0.0055z^2 + 0.0111z + 0.0055}{z^2 - 1.7786z + 0.8008} v_{\text{raw data}}, \tag{1}$$

which has amplitude and phase characteristics as shown in the Bode diagram of Figure 1. This filter is realized in Matlab using the command

```
%2.order Butterworth filter, with normalized bandwidth equal to 0.05
[num,den]=butter(2,0.05);
```

The normalized bandwidth used here, corresponds to

$$w_f = w_{\text{Normalized}} \cdot w_{\text{Nyquist}} = w_{\text{Normalized}} \cdot \frac{\pi}{T} = 0.05 \cdot \frac{\pi}{5} = 0.0314\,\text{rad}/\,\text{s}\,, \tag{2}$$

where w_f is the filter bandwidth, w_{Nyquist} is the Nyquist frequency (the sampling frequency divided by two), $w_{\text{Normalized}}$ is the normalized filter frequency where $w_{\text{Normalized}} = 1$ corresponds to $w_f = w_{\text{Nyquist}}$.

The filtered data are resampled such that the sampling rate used for the model is $T = 30\,\text{s}$. The resampling is carried out simply by picking every 6'th sample from a data set with 5 s sampling rate. Figure 2 shows raw data versus filtered data for an experiment data set collected February 28, 2001.

3 The process model

The process model is described in detail in e.g. (Hauge & Lie 2002) and only a brief description will be given here.

The model was originally developed with several ordinary and partial differential equations. The model was then simplified, and eventually fitted to experimental and operational mill data. The "final" model consists of a third order nonlinear mechanistic model based on physical and chemical laws, and a first order linear empiric

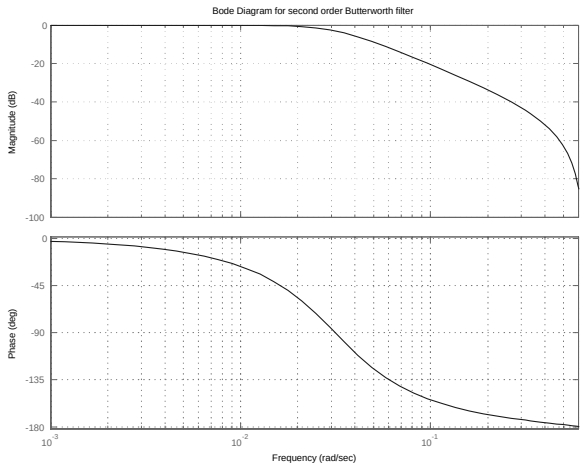

Figure 1: Bode diagram for 2.order Butterworth filter. The cut-off frequency or bandwidth of the filter is 0.0314 rad / s.

model added to the mechanistic model to compensate for neglected and unknown dynamics in the process. The structure of the developed process model is

$$\begin{aligned} \dot{x} &= f(x, u, d, \theta) \\ y &= g(x, u, d, \theta), \end{aligned} \tag{3}$$

with $x \in \mathbb{R}^n = \mathbb{R}^4$, $y \in \mathbb{R}^m = \mathbb{R}^3$, $u \in \mathbb{R}^r = \mathbb{R}^3$ and $d \in \mathbb{R}^d = \mathbb{R}^7$.

The states, manipulated inputs, outputs, and measured disturbances are

$$\begin{aligned} x^T &= [C_{R,fil}, \quad C_{WT,fil}, \quad C_{D,fib}, x_{\text{emp}}] \\ u^T &= [w_{TS}, \quad w_{filler}, \quad w_{\text{ret.aid}}] \\ y^T &= [y_{b.w.}, \quad y_{p.a.}, \quad C_{W,\text{total}}] \\ d^T &= [C_{\text{TS,tot}}, \quad C_{\text{TS,fil}}, \quad S_{\text{1.stage pump}}, \quad v, \quad P, \quad h_{\text{slice}}, \quad f], \end{aligned} \tag{4}$$

where $C_{R,fil}$ is the concentration of filler in a reject tank in the hydrocyclones, $C_{WT,fil}$ is the concentration of filler in the white water tank, $C_{D,fib}$ is the concentration of fiber in the deculator, and x_{emp} is the empiric state added to the mechanistic model to capture neglected and unknown dynamics. The manipulated inputs u are the flow of thick stock, filler, and retention aid. The outputs y are the basis weight, the paper ash content, and the total concentration in the wire tray. The measured disturbances accounted for in the model, are the total and filler thick stock concentrations $C_{\text{TS,tot}}$ and $C_{\text{TS,fil}}$, the speed of a pump between the white water tank and the first stage

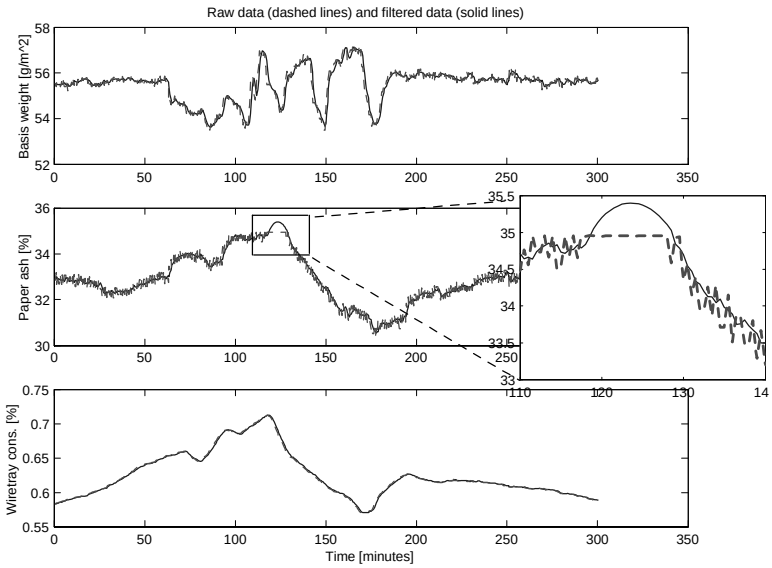

Figure 2: Process outputs during experimentation at February 28, 2001. Raw data, resampled at 30 s sampling rate, are in dashed lines and filtered data, also resampled at 30 s sampling rate, are shown in solid lines. Note the erronous paper ash data near the 125th minute. Cubic interpolation was applied to the data in the erronous region.

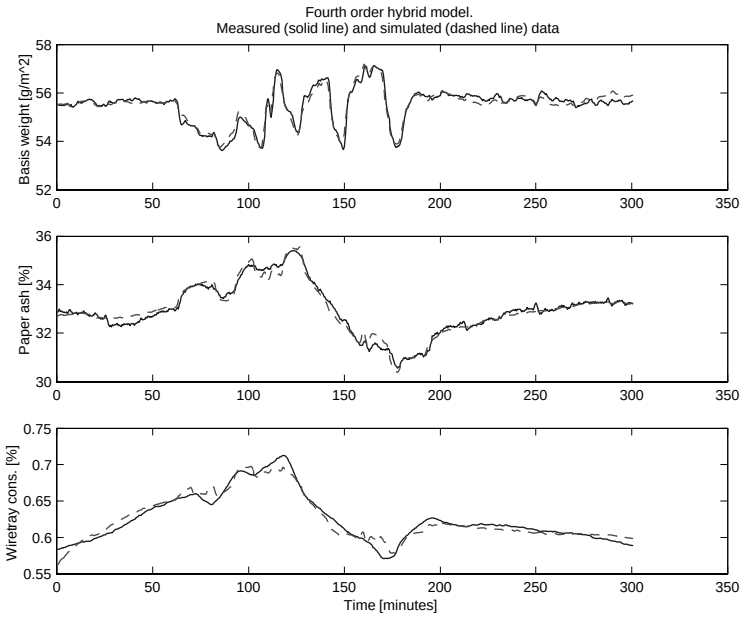

Figure 3: Process model fitted to experimental data.

of the hydrocyclones $S_{1.\text{stage pump}}$, the paper machine velocity v, the pressure inside the headbox P, the mean height of the slice opening h_{slice}, and the paper moisture percentage f.

θ consists of several model parameters, tuned to fit the model outputs to experimental and operational data. In Figure 3, the result from fitting the model to an experimental data set is shown, and Figure 4 shows the validation of the model by comparing simulated model outputs and process measurements during normal operation.

In Figure 5 we have validated the model with a Kalman filter. This Kalman filter is identified from another operational data set, and the filter gain is constant, thus this is a kind of "quasi extended" Kalman filter.

The nonlinear model in Equation 3 is linearized, giving

$$\begin{aligned} x_{k+1} &= Ax_k + Bu_k + Ed_k \\ y_k &= Cx_k + Du_k + Fd_k, \end{aligned} \tag{5}$$

where we for simplicity have used the same variable names as in the nonlinear model[1].

[1] We could e.g. used x^{nonlin} in the nonlinear model, x^o as the operating point, or point of linearization, thus giving the following equation for the linear model variable x^{lin}: $x^{lin} = x^{nonlin} - x^o$.

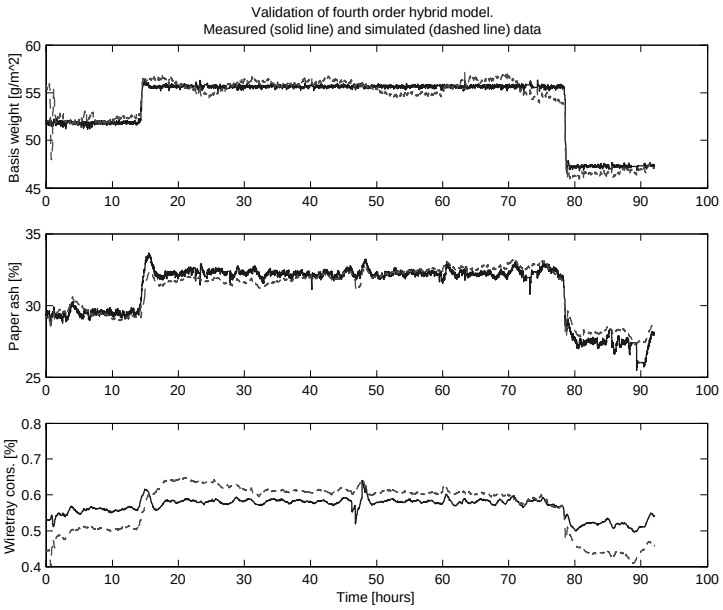

Figure 4: Validation of fourth order process model by simulation. Simulated data are bias corrected.

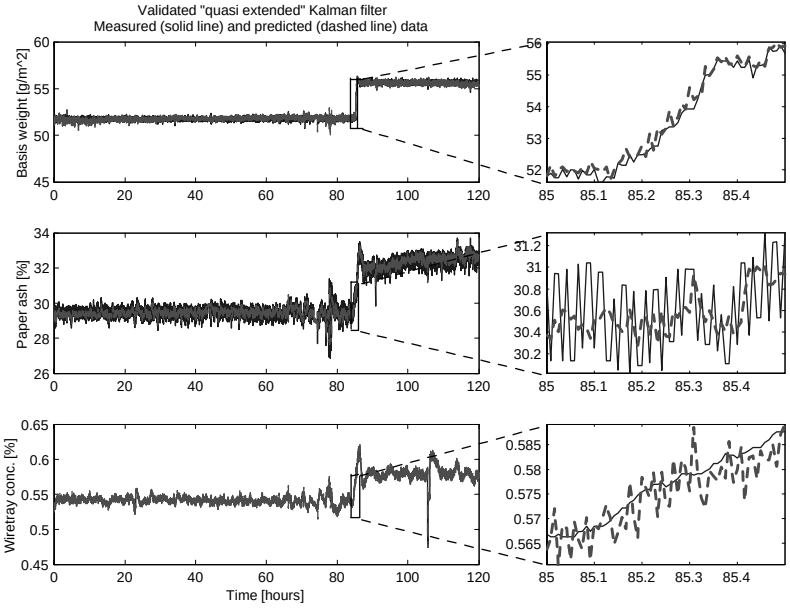

Figure 5: Validation of constant gain Kalman filter. Predictions are bias corrected.

Converting the linear discrete time model to a continuous time model, and then converting to a transfer matrix, we get

$$y(s) = G(s) \cdot u(s) + G_d \cdot d(s), \tag{6}$$

with $G(s) \in \mathbb{R}^{3x3}$ and $G_d(s) \in \mathbb{R}^{3x7}$. In the remainder of this paper we drop the use of the argument s.

4 Controllability

In this section we analyze and discuss the controllability of the paper machine, using techniques for linearized systems. The concept of state controllability will not be discussed, except that we have ascertained that the model is state controllable and observable, and thus a minimal realization. The controllability definition that we will use is one by (Skogestad & Postlethwaite 1996):

Definition 1 *(Input-output) controllability is the ability to achieve acceptable control performance; that is, to keep the outputs (y) within specified bounds or displacements from their references (r), in spite of unknown but bounded variations, such as disturbances (d) and plant changes, using available control inputs (u) and available measurements (y_m, or d_m).*

This concept of controllability is independent of the controller, and is a property of the process alone.

4.1 Model properties

In this subsection we discuss the model properties of the continuous time model, described by the transfer matrix equation 6.

4.1.1 Frequency responses

The frequency responses (magnitudes only) of the elements of G and G_d are shown in Figures 6 and 7. The model is fitted and identified with a direct input to output matrix D, and a direct measured disturbances to output matrix F. The reason for having these "non-physical" direct contributions is that it provided better validation results and model fit. The direct terms are seen on the frequency response plots, giving no roll-off at high frequencies. Some of the responses have their highest gain at higher frequencies, e.g. the response from the third manipulated input. This input is a retention aid, added to help flocculation amongst filler particles and fibers. The step response from this input is shown in Figure 8 and has a clear physical interpretation. The consistency of filler particles and fibers are at a certain level when the step input of retention aid is applied. The flocculation in the pipeline where the retention aid is added, will increase rapidly when the retention aid is increased causing more filler particles and fibers to be retained on the wire, and less to be drained through the

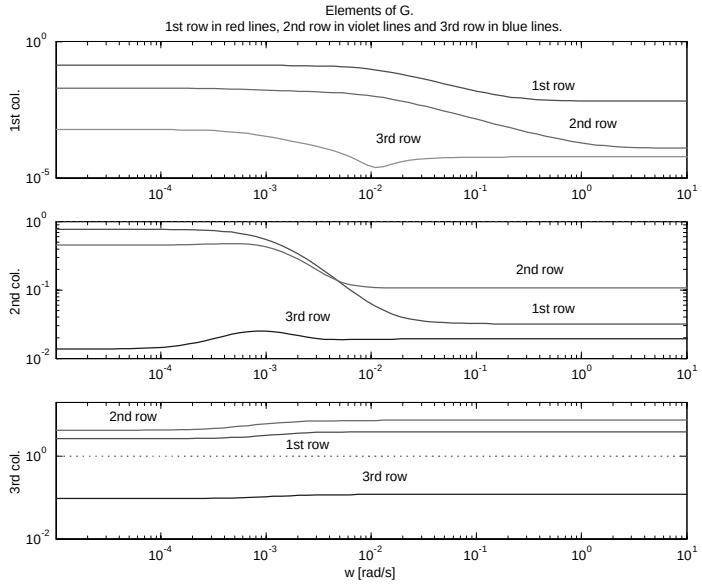

Figure 6: Frequency response of the elements of G. Upper plot is the response from the first column in G, i.e. from the first input to each of the three outputs. The lower plot is the response from the last column in G.

wire. The flow which is drained through the wire is recirculated back into the process and eventually cause a decrease in the consistency in the pipeline where the retention aid is added. This will cause less flocculation, but more flocculation will occur than prior to the step change in input. This means that the magnitude of the frequency response is lower in steady state than at high frequencies.

4.1.2 Poles and zeros

The poles and transmission zeros of the continuos time transfer matrix G (Equation 6) are

$$p = \{-0.0105\ ,\ -0.0038\ ,\ -0.0011\ ,\ -0.0007\}$$
$$z = \{-0.2252\ ,\ -0.0029\ ,\ -0.0013\ ,\ -0.0007\},$$

and we see that G is stable, and has no zeros in the complex right-half plane. G_d has the same poles as G, but has no transmission zeros. Thus, in the absence of right-half plane zeros and poles, we expect no particular controllability problems after studying the poles and transmission zeros.

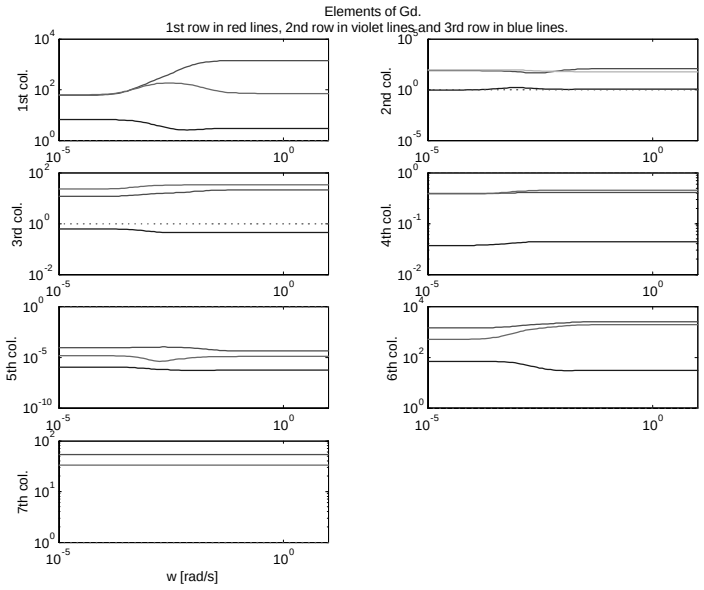

Figure 7: Frequency response of the elements of G_d. Upper left plot is the response from the first column in G_d, i.e. from the first measured disturbance to each of the three outputs.

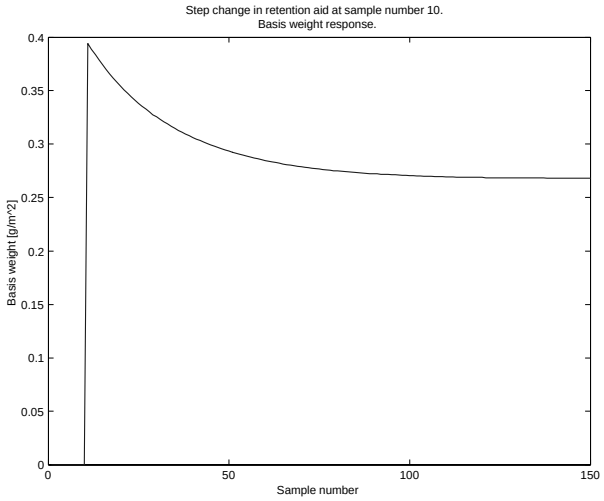

Figure 8: Response in basis weight, after step change in retention aid at the 10'th sample.

4.2 Scaling

To simplify the analysis of controllability with respect to tracking setpoints and suppressing disturbances, we scale the model. The scaling is done so that each input (manipulated input or measured disturbance) is less than one in magnitude, by dividing each variable by its maximum allowed or expected change from its nominal value. Also, the control error, e, and the reference, r, are scaled so that they are allowed to be maximum one in magnitude.

The following scaling matrices are applied

$$\begin{aligned} D_u &= \text{diag}([60\ ,\ 2.4\ ,\ 1.0]) \\ D_d &= \text{diag}([0.006\ ,\ 0.07\ ,\ 0.1\ ,\ 5\ ,\ 0.9 \cdot 10^5\ ,\ 0.0007\ ,\ 0.006]) \\ D_e &= \text{diag}([1.0\ ,\ 1.0\ ,\ 0.05]) \\ D_r &= \text{diag}([10\ ,\ 8\ ,\ 0.15]), \end{aligned} \tag{7}$$

where diag($[\cdot]$) is a diagonal matrix with the elements inside the square brackets on the diagonal. For the manipulated inputs we assume that the maximum allowed changes around the nominal value are ± 60 l / s for the thick stock pump, ± 2.4 l / s for the filler, and ± 1.0 l / s for the retention aid. The measured disturbances are expected to change at maximum ± 0.006 (thick stock total consistency), ± 0.07 (the thick stock filler consistency), ± 0.1 (the first stage pump), ± 5.0 m / s (the paper machine velocity), $\pm 0.9 \cdot 10^5$ Pa (headbox pressure), ± 0.0007 m (slice opening), ± 0.006 % (paper moisture), around the nominal values. The maximum allowed control error

is ± 1.0 g / m^2 for the basis weight, ± 1 % for the paper ash, and ± 0.05 % for the wire tray consistency. The maximum expected reference changes are ± 10 g / m^2 (basis weight), ± 8% (paper ash), and ± 0.15% (wire tray consistency).

In the sequel we denote the scaled transfer matrices by G, and G_d, and the un-scaled original matrices by $\hat{G}$ and $\hat{G}_d$ respectively. The scaled matrices are calculated by

$$G = D_e^{-1}\hat{G}D_u, \;\; G_d = D_e^{-1}\hat{G}_d D_d. \tag{8}$$

Also denote the un-scaled variables by $\hat{e}$, $\hat{y}$, and $\hat{r}$, and we have that

$$\hat{e} = \hat{y} - \hat{r} \implies D_e e = D_e y - D_r r \implies e = y - \underbrace{D_e^{-1} D_r}_{R} r,$$

and the scaled model and variables are

$$y = Gu + G_d d,\; e = y - Rr, \tag{9}$$

where $||u||_\infty \leq 1$, $||d|\,|_\infty \leq 1$, $||e||_\infty \leq 1$, and $||r||_\infty \leq 1$, for the frequencies of interest, and where $||\cdot||_\infty$ is the infinity or max norm (the largest element magnitude in the vector). Thus, the scaling is carried out so that each manipulated input, measured disturbance, control error and reference are less than one in magnitude by dividing each variable by its maximum allowed or expected change from the nominal value.

4.3 Tracking references

In this subsection we discuss the ability to track references, using the scaled continuous time model described by Equation 9

4.3.1 The singular values of the process model

For a given frequency, $G(jw)$ is a constant matrix. The singular value decomposition of $G(jw)$ gives

$$G(jw) = U(jw)S(jw)V^H(jw), \tag{10}$$

where superscript H denotes the conjugate transpose or Hermitian. The matrix $S(jw)$ is diagonal with the singular values in descending order. The largest singular value, $\bar{\sigma}(jw)$, corresponds to the largest gain at frequency w, and the smallest singular value, $\underline{\sigma}(jw)$ corresponds to the smallest gain[2] at frequency w. For a multivariable system, the gain varies with the direction of the input vector, although limited by the largest and smallest singular values. The matrix $U(jw)$ consists of output directions corresponding to the singular values, and $V(jw)$ consists of input directions corresponding to the singular values. Thus, at frequency w, we may find the largest gain as the first singular value, the input direction which gives the largest gain is the first column vector in $V(jw)$, and the output direction as the first column vector in $U(jw)$. Similarly we can find the input and output directions associated with the smallest gain.

[2] This is not true for a system with more inputs than outputs. In this case there will be input directions which will have no affect on the outputs, thus the smallest gain is always zero.

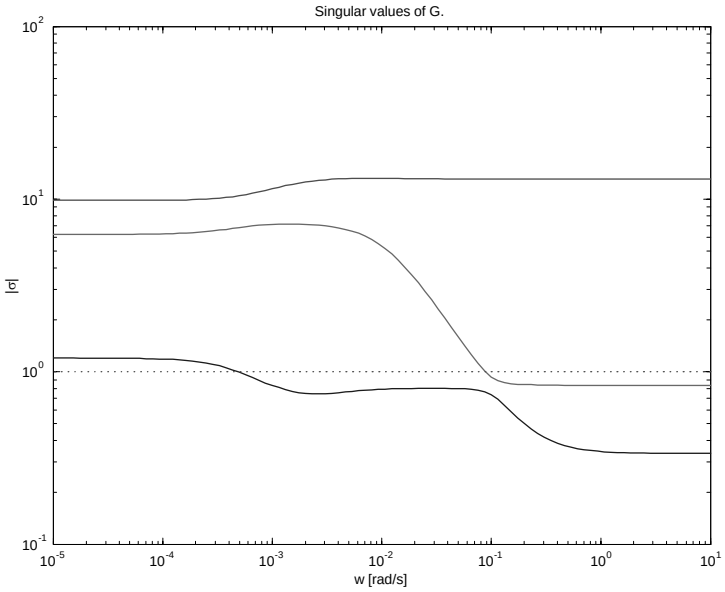

Figure 9: The singular values of G as a function of frequency.

Figure 9 shows the singular values as function of frequency. When the smallest singular value is less than 1, from $6 \cdot 10^{-4}$ rad / s to ∞ rad / s, this means that for some input directions of unit magnitude, the outputs will have less magnitude than one. In general we wish to have the smallest singular value as large as possible, especially within the desired bandwidth of the closed loop system. The singular values are very dependent on the scaling of the model, e.g. if we increase the scaling value for the filler input from 2.4 l / s to 3.4 l / s, then the smallest singular value is larger than one up till 0.1 rad / s. The reason for using 2.4 l / s in the scaling is that this is the operating point where the linear model is derived. Thus increasing the scaling above 2.4 l / s means that we allow a negative flow of filler. However, the physical limits for the filler flow is not symmetric about the operating point, so we may add more filler than the upper scaling limit (which is $2.4 + 2.4 = 4.8$ l / s).

4.3.2 Input saturation

We wish to study if, and at what frequencies, we can obtain perfect reference tracking. Perfect tracking, neglecting the measured disturbances, gives the input

$$\begin{aligned} e &= y - Rr \\ &\Downarrow \\ 0 &= Gu - Rr \\ &\Downarrow \\ u &= G^{\dagger}Rr, \end{aligned} \tag{11}$$

where $G^{\dagger} = G^H(GG^H)^{-1}$ is the pseudo-inverse. Figure 10 shows the frequency response of the elements of $G^{\dagger}R$ (magnitudes only). At frequencies were the magnitude exceeds one, we cannot achieve perfect tracking because $||u||_{\infty} = \left||G^{\dagger}Rr|\right|_{\infty} \leq 1$ is not satisfied for all $||r||_{\infty} \leq 1$. Note that we here study the references one by one, and not by means of e.g. a worst case scenario for all involved references.

The first column of $G^{\dagger}R$ corresponds to tracking the basis weight setpoint. In Figure 10 we see that none of the inputs saturate in steady state, however the element in the first row exceeds one in magnitude at a too low frequency. In the second and third columns of $G^{\dagger}R$ wee see that the elements in the second row are above one at all frequencies. Thus, we expect that the filler valve will saturate when operating in the outer regions of the paper ash and wire tray consistency setpoints.

The notion of a plant that can not be perfectly controlled, is even more clear if we study a combined reference change, limited by $||r(jw)||_2 \leq 1$, and $||u(jw)||_2 \leq 1$. The maximum expected reference change is ± 1 for each reference, and the maximum allowed input change is ± 1 for each input, however the limitations introduced here simplifies the calculation and is convenient for illustrating our main point: that the measured disturbances must be monitored, adjusted and related to the reference values. Using Equation 11 and the above limitation for u, we can write

$$\begin{aligned} ||u||_2 &= \left||G^{\dagger}Rr|\right|_2 \leq 1 \\ &\Downarrow \\ ||u||_2 &= \left||G^{\dagger}R|\right|_{i2} \cdot ||r||_2 \leq 1, \end{aligned} \tag{12}$$

where $||\cdot||_{i2}$ is the induced 2-norm, or the largest singular value. For $||r||_2 = 1$ we have that

$$\bar{\sigma}(G^{\dagger}R) \leq 1, \tag{13}$$

for perfect reference tracking, without input saturation. Figure 11 shows the singular values of $G^{\dagger}R$ plotted as function of frequency, and it is clear that perfect tracking is not obtained at any frequency with large combined reference changes.

Some comments on these results are necessary. First, for higher frequencies we will not expect nor want perfect tracking in most cases (large and rapid actuator movements). Based on knowledge of the process, it is expected that the bandwidth

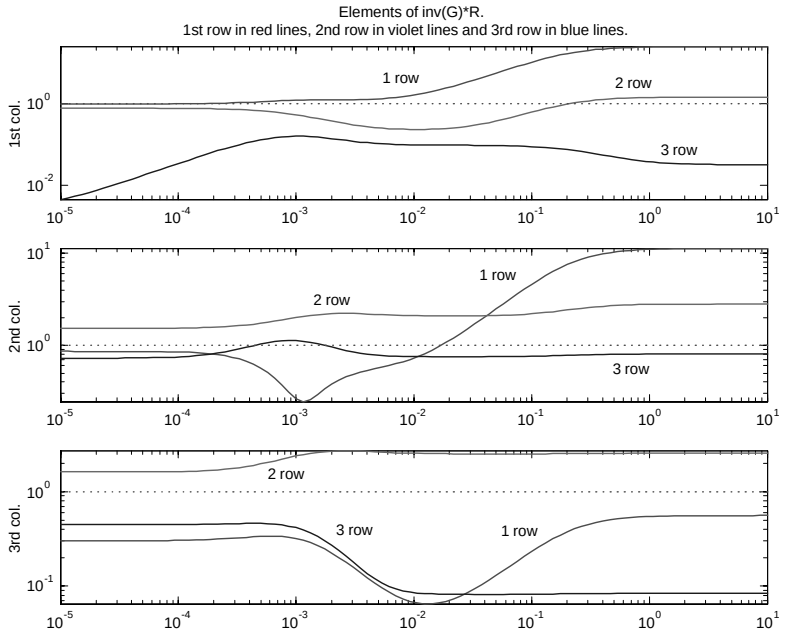

Figure 10: Magnitudes of the frequency response of the elements of $G^{\dagger}R$.

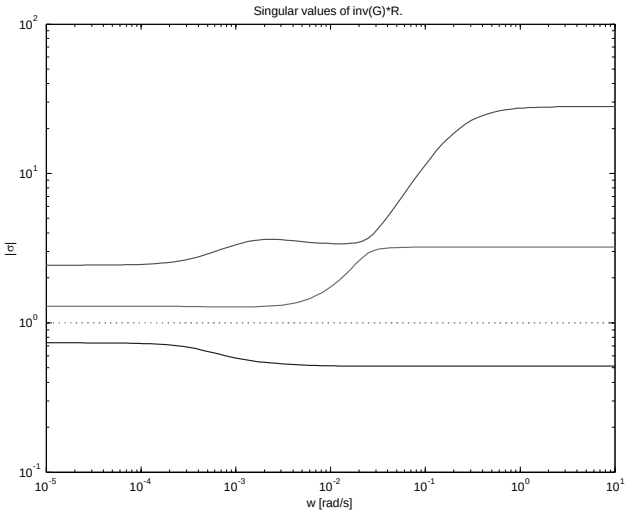

Figure 11: Singular values of $G^{\dagger}R$, as a function of frequency.

of the closed loop system should be around 0.01 - 0.1 rad/s. Second, for lower frequencies, at least for steady state conditions, one would normally expect to obtain perfect control. However, knowing that we neglected the measured disturbances in this particular analysis, we probably have a good explanation of the result in Figure 4. The conditions were the linearization was carried out was e.g. 50 g/m2 basis weight, 30% paper ash, 4% thick stock total consistency, and 1.48% thick stock filler consistency. The scaling of the model is carried out so that the entire product range of PM6 is reflected, e.g. the paper ash content can be as low as 20%. Given that the filler content in the thick stock is approximately 37%, as is the case here, the manipulated inputs would most certainly saturate trying to reach a paper ash level of 20%.

The comments above are supported by the fact that there are no known input saturation problems at PM6 today, however the process operators carefully adjusts e.g. thick stock consistencies to match the specifications on the finished paper. This analysis shows that without these adjustments from the process operators, off-spec paper would be produced. This would be the case independent of the controller which is used.

4.4 Rejecting disturbances

The model is scaled so that each disturbance should be less than one (absolute value), and we have also scaled the model with the allowed output error $(r-y)$. The frequency response of G_d will then show whether we need control or not, by studying the gain

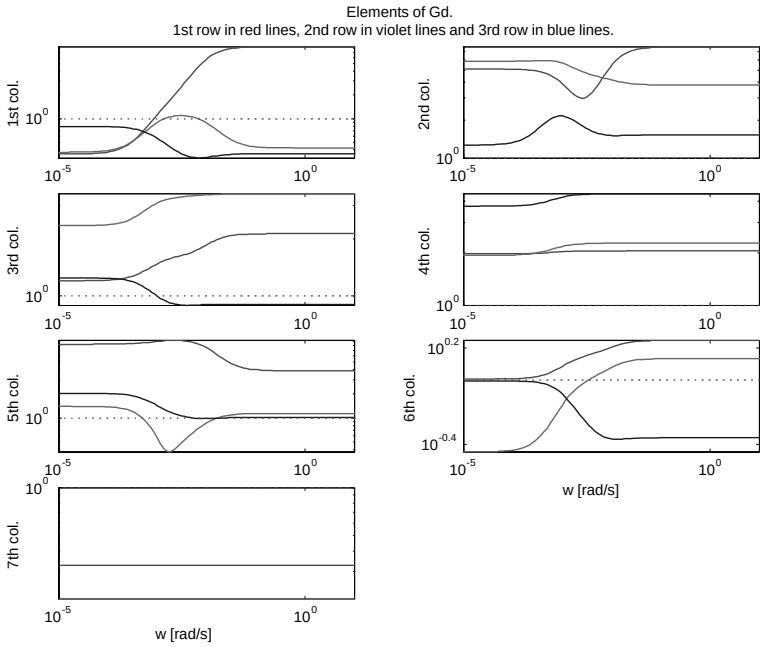

Figure 12: Magnitude of the frequency response of the elements of G_d.

from each disturbance to each output. At frequencies where the gain is larger than one, we need control. From Figure 12 we see that for most of the disturbances we need control, while the paper moisture disturbance, described by the seventh column in G_d, we do not need control in order to stay within the allowed control errors. We also see that for many of the disturbances we need control at high frequencies, however it is beyond the scope of most control loops to reject disturbances at very high frequencies.

4.4.1 Input saturation

Perhaps more interesting is the question of whether we can reject disturbances, while still maintaining acceptable manipulated inputs. Let us look at the possibility of achieving perfect control. That is, given some disturbance, can we keep $||e||_{\max} = 0$, and still maintain $||u||_{\max} \leq 1$? For simplicity, and without loss of generality, we set

$r = 0$

$$\begin{aligned} r - y &= r - Gu - G_d d \\ &\Downarrow \\ 0 &= Gu + G_d d \\ &\Downarrow \\ u &= -G^{\dagger} G_d d, \end{aligned}$$

and this is the input required for perfect control.

Figure 13 shows the frequency response of the elements of $G^{\dagger}G_d$ (magnitudes only). From this figure we see which disturbances can be controlled perfectly at which frequencies. Note that here we study the disturbances one by one, and not by means of e.g. a worst case scenario for all involved disturbances. For example in the upper left figure are the responses of the first column of $G^{\dagger}G_d$, corresponding to the first disturbance which is the thick stock total consistency. At low frequencies we see that the magnitudes are below one, which means that the outputs can be controlled perfectly even for a worst case disturbance in the thick stock total consistency (assuming other disturbances are zero). At higher frequencies the magnitude of the basis weight response (first row) crosses the saturation line (dashed line at magnitude equal to one), and at even higher frequencies the paper ash also exceeds one in magnitude. At frequencies were the magnitude exceeds one, we cannot achieve perfect control because $||u||_{\infty} = \left|\left|G^{\dagger}G_d d\right|\right|_{\infty} \leq 1$ is not satisfied for all $||d||_{\infty} \leq 1$.

In Figure 13 we do not worry very much about the higher frequencies, as we would not expect to achieve perfect control here any way. What is interesting is those cases where we have magnitudes larger than one, at lower frequencies. These are in particular the responses in the second column and second row, the fourth column and the second row, and the fifth column and the second row (referring to columns and rows in $G^{\dagger}G_d$). Consider e.g. the thick stock filler consistency (the second disturbance) and the inability to achieve perfect control of the paper ash even in steady state, as can be seen in the upper right corner in Figure 13. The paper ash originates from filler in the thick stock and filler added in the short circulation (the second manipulated input). The process operators make sure that when a high percentage of paper ash is required, then a high percentage of filler in the thick stock is present. Similarly, when a low paper ash percentage is required, then a lower percentage of filler is present in the thick stock. Thus, it is our opinion that the inability to achieve perfect control in steady state is a problem that is solved by the process operators. What can be learned here, is that in order to track the setpoints, also at low frequencies, it is necessary to either manually or automatically be able to influence some of the measured disturbances. As of today the process operators carefully adjust e.g. the thick stock composition to match the specifications on the finished paper, and without these adjustments off-spec paper would be produced as shown in Figure 13.

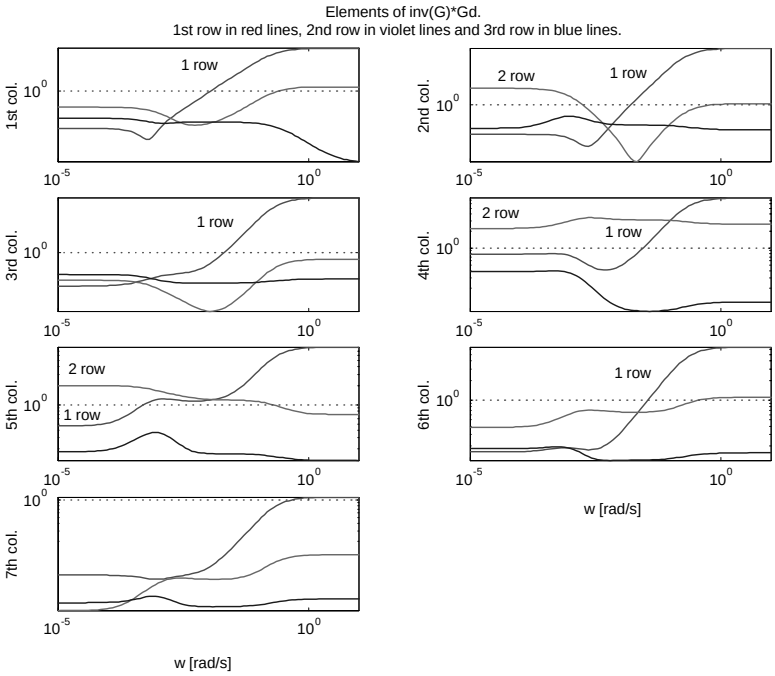

Figure 13: Magnitudes of the frequency response of the elements of $G^{\dagger}G_d$.

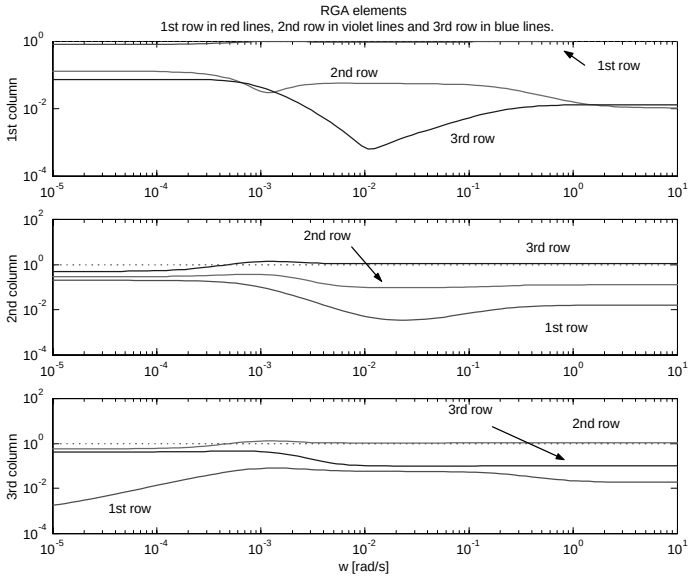

Figure 14: Frequency response of the RGA elements (only magnitudes), $\Lambda(G)$.

4.5 Sensitivity to uncertainty

4.5.1 Relative Gain Array (RGA)

The RGA is perhaps best known as a way to choose pairing between inputs and outputs for decentralized control. However, it also has an important application as an indicator of sensitivity to uncertainty (Skogestad & Postlethwaite 1996). The RGA is defined as

$$\Lambda(G) = G \times \left(G^{\dagger}\right)^{T}, \tag{14}$$

where $\times$ is the Hadamard product (an element by element multiplication). Figure 14 shows the frequency responses (only magnitudes) of the elements of the RGA matrix. Processes with large RGA elements (e.g. magnitude above 10) are fundamentally difficult to control due to sensitivity to input uncertainty (Skogestad & Postlethwaite 1996). Based on the frequency responses of Figure 14, there is no indication of such problems for the paper machine process.

It is interesting to note that the present choice of input-output pairing for decentralized control in the industry is not the choice that would be made based on the RGA frequency response. The rules of thumb for pairing are often given as: Choose pairing so that the corresponding RGA elements

1. in steady state, $\Lambda(G(0))$, are positive and as close to 1 as possible (Skogestad & Postlethwaite 1996).

2. near the desired bandwidth of the closed loop system, $\Lambda(G(w_b))$, are as close to 1 as possible (Skogestad & Postlethwaite 1996) (Seborg, Edgar & Mellichamp 1989).

In Figure 14 we see in the upper figure that we would choose to pair the thick stock pump (input 1) with the basis weight (output 1). This corresponds to the choice made in the industry. However, for the filler valve input (figure in the middle) we would choose to pair it with the wire tray consistency (output 3), and finally for the retention aid input (lower figure) we would choose to pair it with the paper ash (output 2). These last two pairings are not in correspondence with the industrial choice, as known by the authors of this paper.

4.5.2 Condition number

The condition number of the process is defined as

$$\gamma(G) = \frac{\bar{\sigma}(G)}{\underline{\sigma}(G)}, \tag{15}$$

and is an indicator of sensitivity to both diagonal and full-block input uncertainty (Skogestad & Postlethwaite 1996). A small condition number indicates robustness to the uncertainty. Figure 15 shows the condition number as a function of frequency. A rule of thumb states that a condition number larger than 10 may indicate sensitivity to uncertainty. In our case we do not expect very much sensitivity at lower frequencies, however at frequencies ranging from 10^{-3} to 10^{-1} rad / s there may be a problem with sensitivity to input uncertainty.

5 APIS (Advanced Process Improvement System)

APIS consists of a number of software components for process control, process data logging and presentation of process information on web pages, e.g. Apis MPC and Apis SoftSensor (a Kalman filter). Apis is a product of Prediktor AS (Norway) and more information is available at the company homepage at www.prediktor.no.

5.1 The "standard" APIS Model Predictive Controller (MPC)

The Apis MPC is based on an algorithm presented in (Muske & Rawlings 1993), although there are some modifications and extensions based on experience from MPC in industrial applications. The model is a linear state space model similar to Equation 5, with the following infinite horizon quadratic objective function

$$J_k = \sum_{j=0}^{\infty} \left[(y_{k+j} - y_s)^T Q (y_{k+j} - y_s) + (u_{k+j} - u_s)^T R (u_{k+j} - u_s) + \Delta u_{k+j}^T S \Delta u_{k+j} \right], \tag{16}$$

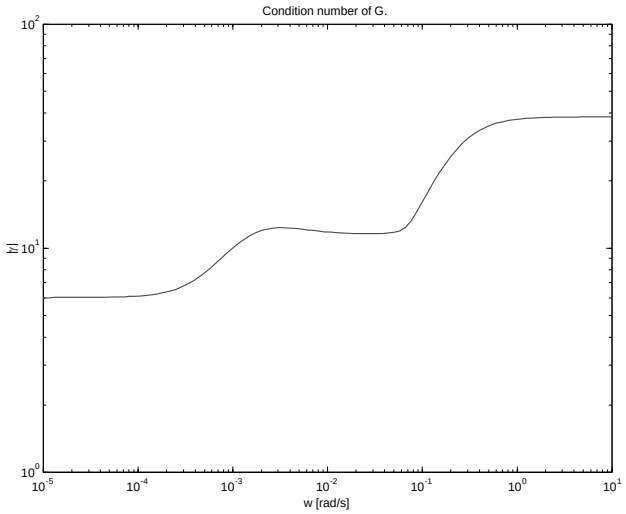

Figure 15: Condition number of G.

where $\Delta u_{k+j} = u_{k+j} - u_{k+j-1}$, y_s and u_s are target vectors for the inputs and outputs, Q and R are positive definite penalty matrices, and S is a positive semidefinite penalty matrix.

The MPC is based on minimization of the criterion subject to specified constraints. The model in Equation 5 gives a set of equality constraints, while the inequality constraints are

$$\begin{aligned} u_{\min} \leq u_{k+j} \leq u_{\max}, \;\; j = 0, 1, 2, ..., N-1 \\ y_{\min} \leq y_{k+j} \leq y_{\max}, \;\; j = j_1, j_1+1, ..., j_2 \\ \Delta u_{\min} \leq \Delta u_{k+j} \leq \Delta u_{\max}, \;\; j = 0, 1, 2, ..., N, \end{aligned} \tag{17}$$

where N is the horizon after which no control moves are allowed, and $[k+j_1, k+j_2]$ are the time interval where the output constraints are applied. The criterion is of infinite horizon, and this guarantees stability. Through the use of a Lyapunov equation the criterion can be reformulated as a finite horizon criterion which can be implemented.

5.2 A modified MPC for APIS

The APIS MPC described in the previous section can not handle nonlinear models or future setpoint changes. A modified MPC which handles these issues, is therefore currently being developed and implemented. The nonlinear model is linearized at each sample and used in the MPC.

At time k, suppose a reference vector and a measured disturbance vector for time $k, k+1, ..., k+N-1$ is given. These vectors may be provided by the process operators or simply taken as an expansion of the present values into the future. Using the linearized model at time k (as given by Equation 5) we calculate feasible target values at each sample up till $k+N-1$. The model of Equation 5, is then shifted, so that the origin of the model is the target value at time $k+N-1$. The shifted values are denoted by a bar (e.g. $\bar{x}$) in the remainder of this paper.

Assuming no control moves beyond sample $k+N-1$, and no change in target values beyond sample $k+N-1$, we can reformulate the infinite horizon criterion to the following finite horizon criterion

$$\begin{aligned} J_k = {} & \bar{x}_{k+N}^T \bar{Q}_k \bar{x}_{k+N} - 2\bar{u}_{k-1}^T S \bar{u}_k - \sum_{j=1}^{N-1} \left[2\bar{u}_{k+j}^T S \bar{u}_{k+j-1} \right] \\ & + \sum_{j=0}^{N-1} \left[\bar{y}_{k+j}^T Q \bar{y}_{k+j} - 2\left(\bar{y}_{k+j}^s\right)^T Q \bar{y}_{k+j} + \bar{u}_{k+j}^T \left(R+2S\right) \bar{u}_{k+j} - 2\left(\bar{u}_{k+j}^s\right)^T R \bar{u}_{k+j} \right] \\ & + \text{constant}\,. \end{aligned} \tag{18}$$

where $\bar{Q}$ is the solution of a Lyapunov equation, and the vector of unknowns is

$$z^T = \left[\bar{u}_k^T, \bar{u}_{k+1}^T, ..., \bar{u}_{k+N-1}^T, \bar{x}_{k+1}^T, \bar{x}_{k+2}^T, ..., \bar{x}_{k+N}^T, \bar{y}_k^T, \bar{y}_{k+1}^T, ..., \bar{y}_{k+N-1}^T \right], \tag{19}$$

The constraints are given by Equations 5 and 17. It is possible to reduce the number of unknowns in the z vector by inserting the model equations in the criterion. However, the formulation given here gives very sparse matrices, and sparse solvers quickly solve the optimization problem. Which method is more efficient is not studied in this paper.

6 A simulation result

For the process operators at PM6, the MPC will include some options not available previously. These include making future reference changes, control during sheet breaks and control during start up. The inclusion of the non-linear model in the controller makes it possible to rely on the model output when measurements are not available such as during start up and sheet breaks. The possibility of making future reference changes means that the controller can prepare the inputs and states for the forthcoming change, and calculate an optimal grade change. In Figure 16 the simulated outputs are shown, when the change in reference values is submitted to the MPC 50 minutes before the actual grade change.

For the simulation in Figure 16, control deviation caused by the basis weight is penalized hard, while the control deviation caused by the wire tray consistency is penalized relatively mild. Both the control increment (Δu) and the control deviation from the steady state value is penalized in the criterion. The control increment is

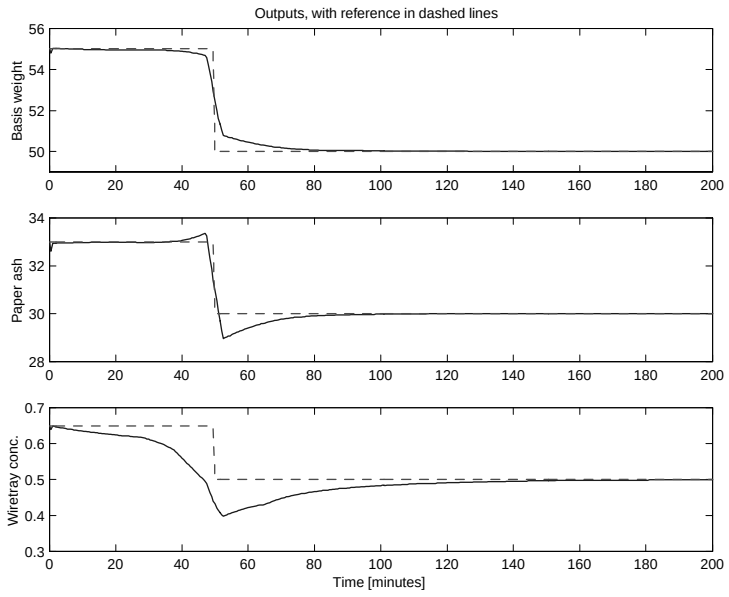

Figure 16: Model outputs and reference values (in dashed lines). The change in reference value at $t = 50$ minutes was submitted to the MPC at $t = 0$ minutes.

constrained by ± 2 liters per sample (the sampling time is 30 seconds) for the thick stock, ± 0.25 liters per sample for filler, and ± 0.05 liters per sample for the retention aid.

7 Conclusions

In this paper we gave a preliminary analysis of a developed paper machine model and its use in an MPC application. The process is non-linear and the analysis is carried out on a linearized model.

There are no strong indications of expected control problems, although the process to some extent may be sensitive to uncertainty. Input saturation may occur for large changes in disturbances and references. However, this can probably be compensated for by the process operators acting on measured disturbances (as is done today at PM6). A simulation result with a modified commercially available MPC algorithm is shown. The modifications include e.g. allowing future setpoint changes.

Acknowledgements The authors would like to thank the employees at PM6 for their cooperation in providing information and data for this paper, and for their general helpfulness. Steinar Sælid and Anders Veberg from Prediktor AS is acknowledged for information about APIS and APIS MPC. The work of Tor Anders Hauge is financially supported by the Research Council of Norway (project number 134557/432), with additional financial support by Norske Skog Saugbrugs.

References

Hauge, T. A., Ergon, R., Forsland, G. O., Slora, R. & Lie, B. (2000), Modeling, Simulation and Control of Paper Machine Quality Variables at Norske Skog Saugbrugs, Norway, *in* 'Scientific and Technological Advances in the Measurement and Control of Papermaking', Pira International.

Hauge, T. A. & Lie, B. (2002), 'Paper machine modeling at Norske Skog Saugbrugs: A mechanistic approach', *Modeling, Identification and Control* **23**(1), 27–52.

Muske, K. R. & Rawlings, J. B. (1993), 'Model predictive control with linear models', *AIChE Journal* **39**(2), 262–287.

Seborg, D. E., Edgar, T. F. & Mellichamp, D. A. (1989), *Process Dynamics and Control*, John Wiley & Sons, Inc.

Skogestad, S. & Postlethwaite, I. (1996), *Multivariable Feedback Control: Analysis and Design*, John Wiley & Sons Ltd.